

Organic Light-Emitting Diodes

2,5-Difluorenyl-Substituted Siloles for the Fabrication of High-Performance Yellow Organic Light-Emitting Diodes

Bin Chen,^[a] Yibin Jiang,^[c] Long Chen,^[b] Han Nie,^[b] Bairong He,^[a] Ping Lu,^[e] Herman H. Y. Sung,^[d] Ian D. Williams,^[d] Hoi Sing Kwok,^[c] Anjun Qin,^[b] Zujin Zhao,^{*,[a, b]} and Ben Zhong Tang^{*,[b, d]}

Abstract: 2,3,4,5-Tetraarylsiloles are a class of important luminogenic materials with efficient solid-state emission and excellent electron-transport capacity. However, those exhibiting outstanding electroluminescence properties are still rare. In this work, bulky 9,9-dimethylfluorenyl, 9,9-diphenylfluorenyl, and 9,9'-spirobifluorenyl substituents were introduced into the 2,5-positions of silole rings. The resulting 2,5-difluorenyl-substituted siloles are thermally stable and have low-lying LUMO energy levels. Crystallographic analysis revealed that intramolecular π - π interactions are prone to form between 9,9'-spirobifluorene units and phenyl rings at the 3,4-positions of the silole ring. In the solution state, these new siloles show weak blue and green emission bands, arising from the fluorenyl groups and silole rings with a certain ex-

tension of π conjugation, respectively. With increasing substituent volume, intramolecular rotation is decreased, and thus the emissions of the present siloles gradually improved and they showed higher fluorescence quantum yields ($\Phi_F = 2.5$ –5.4%) than 2,3,4,5-tetraphenylsiloles. They are highly emissive in solid films, with dominant green to yellow emissions and good solid-state Φ_F values (75–88%). Efficient organic light-emitting diodes were fabricated by adopting them as host emitters and gave high luminance, current efficiency, and power efficiency of up to 44 100 cd m^{-2} , 18.3 cd A^{-1} , and 15.7 lm W^{-1} , respectively. Notably, a maximum external quantum efficiency of 5.5% was achieved in an optimized device.

Introduction

Design and synthesis of solid-state luminescent materials are of academic and practical significance, because many popular dyes that show good fluorescence in solution become weak emitters when assembled as nanoparticles or fabricated into

solid films. This emission-quenching effect, known as aggregation-caused quenching (ACQ), remains a difficult problem to tackle. New luminogens that act contrarily would be highly desirable. The phenomenon of aggregation-induced emission (AIE) was discovered in certain compounds, such as siloles,^[1] cyanostilbenes,^[2] tetraphenylethenes,^[3] diphenyldibenzofulvenes,^[4] and phosphole oxides.^[5] This important finding helps to alleviate the ACQ problem and paves a new avenue to create efficient solid-state emitters. Many luminogenic materials with AIE-active units exhibit high fluorescence efficiencies in solid films and show great potential in optoelectronic devices, such as organic light-emitting diodes (OLEDs).^[6,7]

In the past two decades, siloles have received considerable research attention, and various silole-based functional materials were developed. Amongst them, propeller-like 2,3,4,5-tetraphenylsiloles, such as 1-methyl-1,2,3,4,5-pentaphenylsilole (MPPS) and 1,1-dimethyl-2,3,4,5-tetraphenylsilole (DMTPS), were the first AIE luminogens, reported by Tang et al. in 2001 (Scheme 1).^[1a] These luminogens are almost nonfluorescent in the solution state but turned out to be strong emitters in the aggregated state. Their abnormal emission behaviors were rationalized by restriction of intramolecular rotation in the condensed phase.^[8] The AIE property enables efficient emission of these siloles in solid films and their use as light emitters in OLEDs.^[9,10] In addition, siloles are interesting σ^* - π^* conjugated molecules. The interaction between the σ^* orbital of the silicon-carbon bond and the π^* orbital of the butadiene segment

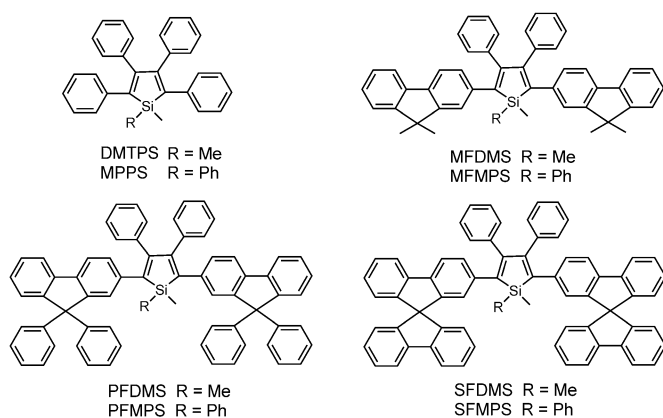
[a] B. Chen, B. He, Prof. Z. Zhao
College of Material, Chemistry and Chemical Engineering
Hangzhou Normal University
Hangzhou 310036 (China)
E-mail: zujinzhao@gmail.com

[b] L. Chen, H. Nie, Prof. A. Qin, Prof. Z. Zhao, Prof. B. Z. Tang
Center for Display Research
State Key Laboratory of Luminescent Materials and Devices
South China University of Technology
Guangzhou 510640 (China)

[c] Y. Jiang, Prof. H. S. Kwok
Center for Display Research
The Hong Kong University of Science & Technology (HKUST)
Kowloon, Hong Kong (China)

[d] H. H. Y. Sung, Prof. I. D. Williams, Prof. B. Z. Tang
Department of Chemistry, Division of Biomedical Engineering
Institute for Advanced Study and Institute of
Molecular Functional Materials
HKUST, Kowloon, Hong Kong (China)
E-mail: tangbenz@ust.hk

[e] Dr. P. Lu
State Key Laboratory of Supramolecular Structure and Materials
Jilin University, Changchun 130012 (China)



Scheme 1. Molecular structures of 2,3,4,5-tetrafluorenylsiloles and 2,5-difluorenyl-substituted siloles.

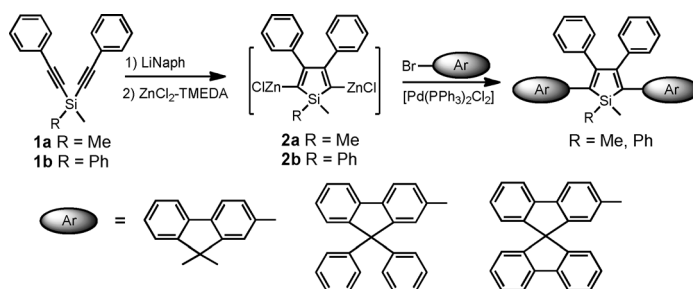
leads to a low-lying LUMO energy level, and thus endows siloles with high electron affinity and high electron mobility. They can outperform widely used electron-transporting materials such as tris(8-hydroxyquinolino)aluminum (Alq_3) in OLEDs.^[11]

Whereas siloles are good solid-state emitters and electron transporters, most OLEDs based thereon afford moderate external quantum efficiencies of about 3% or less. Only a few silole-based OLEDs show excellent performance with high external quantum efficiencies close to the theoretical limit.^[12] With this in mind, we sought new silole emitters by molecular engineering. In this work, a series of tailored 2,5-difluorenyl-substituted siloles (Scheme 1) were designed and synthesized. Different-sized fluorenyl substituents were incorporated into the silole rings in order to systematically study the photoluminescence (PL) properties of the resulting luminogens. Such bulkily substituted siloles^[13] are rarely prepared, probably due to the synthetic difficulties arising from steric hindrance. It was envisioned that the bulky substituents may affect the intramolecular rotation of the aromatic rotors around the silole rings and thus change their AIE characteristics. Applications of these new siloles as light emitters for OLEDs were investigated. Efficient undoped OLEDs were fabricated that exhibit remarkably high current, power, and external quantum efficiencies of up to 18.3 cd A^{-1} , 15.7 lm W^{-1} , and 5.5%, respectively.

Results and Discussion

Synthesis

Scheme 2 illustrates the synthetic route to 2,5-difluorenyl-substituted siloles. Starting materials **1a** and **1b** were prepared by literature methods.^[9b] The *endo-endo* intramolecular reductive cyclization of **1** in the presence of lithium naphthalenide to generate 2,5-dilithiosiloles was followed by treatment with $\text{ZnCl}_2 \cdot \text{TMEDA}$ to yield 2,5-dimetallated silole intermediates **2**.^[11a] Palladium-catalyzed cross-coupling of **2** with 2-bromo-9,9-dimethylfluorene, 2-bromo-9,9-diphenylfluorene, or 2-bromo-9,9'-spirobifluorene furnished target siloles with different-sized fluorenyl substituents at the 2,5-positions. Although 9,9-diphe-



Scheme 2. Synthetic route to 2,5-difluorenyl-substituted siloles. LiNaph = lithium naphthalenide, TMEDA = *N,N,N',N'*-tetramethylethylenediamine.

nylfuorenyl and 9,9'-spirobifluorenyl are rather bulky groups, they were successfully incorporated into the 2,5-positions of the silole ring. PFDMS and SFDMS were obtained in moderate yields of 44 and 45%, respectively, which are only slightly lower than those of MFMPs (50%) and MFDMS (58%). The yields of PFMPs and SFMPs, however, were only 26 and 22%, respectively, because spatial congestion from the substituent at the 1-position prevents the bulky groups from getting close to the silole ring and thus reduces the reaction yields. All these silole products were characterized by spectroscopic methods and elemental analysis. They are soluble in common organic solvents including THF, dichloromethane, chloroform, and toluene, but insoluble in water and methanol. The thermal stability was evaluated by thermogravimetric analysis (TGA). As shown in Figure 1, these new siloles have good thermal stability and high decomposition temperatures T_d in the range of 301–404 °C (Table 1) for 5% loss of initial weight. Thus, their thermal stability is high enough for film fabrication by vapor deposition.

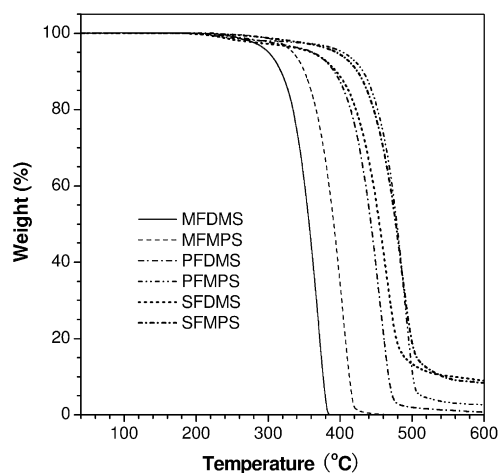


Figure 1. Thermogravimetric analysis of 2,5-difluorenyl-substituted siloles under nitrogen at a heating rate of $10^\circ\text{C min}^{-1}$.

Crystal structures

Single crystals of MFDMS, MFMPs, PFMPs, SFDMS, and SFMPs were grown from THF/ethanol and analyzed by X-ray diffraction crystallography. Their crystal structures are shown in Figure 2. Introducing bulky substituents such as 9,9'-spirobi-

Table 1. Optical and thermal properties of 2,5-difluorenyl-substituted siloles.

	λ_{abs} [nm] solution ^[a]	λ_{em} [nm] solution ^[a]	film ^[b]	Φ_{F} [%] solution ^[c]	film ^[d]	T_{d} [°C]
MFDMS	396	412, 434, 506	523	2.5	75	301
MFMPs	401	411, 435, 512	534	2.6	88	334
PFDMS	391	419, 439, 502	522	3.3	80	362
PFMPs	399	414, 434, 515	533	5.4	86	404
SFDMS	397	417, 436, 503	521	5.0	85	360
SFMPs	402	415, 435, 507	535	4.8	76	395

[a] In THF solution (10 μM). [b] Drop-cast film on quartz plate. [c] Fluorescence quantum yields determined in THF solutions with 9,10-diphenylanthracene ($\Phi_{\text{F}}=90\%$ in cyclohexane) as standard. [d] Fluorescence quantum yields of the amorphous films measured by integrating sphere.

fluorenyl and 9,9-diphenylfluorenyl at the 2,5-positions of silole rings results in highly congested molecules. The aromatic rings at the 9,9-positions of fluorene rings closely approach the phenyl rings at the 3,4-positions of the silole rings, so that intramolecular π - π interactions become possible. For instance, in SFDMS and SFMPs, fluorene and phenyl rings at the 3,4-positions of silole rings are arranged in a nearly parallel manner with shortest inter-ring distances ranging from 3.458 to 3.801 Å (Figure 2). Such a conformation allows intramolecular π - π interactions between the fluorene and phenyl rings. Thus, the rigidity of the molecules is reinforced and intramolecular rotation is reduced. The volumes of the substituents at the 2,5-positions also have great impact on the molecular packing of the molecules in the crystalline state. For example, MFMPs molecules are arranged in a more regular manner than PFMPs molecules in the crystal (Figure 3). The molecules of MFMPs can get much closer than those of PFMPs, due to less spatial congestion of a 9,9-dimethylfluorenyl compared to a 9,9-diphenylfluorenyl group. The tight and regular packing of the molecules is conducive to charge transport and thus device performance.

Optical properties

Figure 4 shows the absorption spectra of the 2,5-difluorenyl-substituted siloles in dilute THF solutions. The absorption maximum of MFMPs, associated with the π - π^* transition, is located at 401 nm, which is slightly redshifted by 5 nm relative to that of MFDMS (396 nm). Similar small redshifts are also observed on comparing the absorption spectra of PFDMS and PFMPs, as well as those of SFDMS and SFMPs (Table 1). These findings agree with our previous observations on silole derivatives, and are attributed to the inductive effect^[11b,14] of the additional phenyl rings at the 1-position of silole rings. MFMPs shows a main emission band peaking at 512 nm. In addition, two blue emission bands at about 411 and 435 nm are present. Similar blue emission bands were also detected for the other 2,5-difluorenyl-substituted siloles besides the long-wavelength emission bands (Table 1). Since intramolecular rotation of aromatic substituents with respect to silole rings is active in the solution state, the electronic and energetic communication between fluorenyl substituents and silole ring is impaired by such motions. Thus, it is deduced that the blue emissions mainly originate from the fluorenyl segments, as were also observed for other AIE-active small molecules^[15] and conjugated polymers.^[16] The long-wavelength emission stems from the silole rings with a certain extension of the π conjugation. The PL emissions of these new siloles are weak in dilute THF solutions, with low fluorescence quantum yields Φ_{F} of 2.5–5.4%, because the intramolecular rotation deactivates the excited state in a nonradiative pathway. The Φ_{F} values increase progressively with increasing substituent volume and become much higher than those of 2,3,4,5-tetraphenylsiloles (e.g., MPPS, 0.09%) and other siloles in the literature.^[1,9b] This should be due to the reduced intramolecular rotation owing to the spatial constraint of the bulky groups and reinforced stiffness of the molecules.^[6e,13a,17]

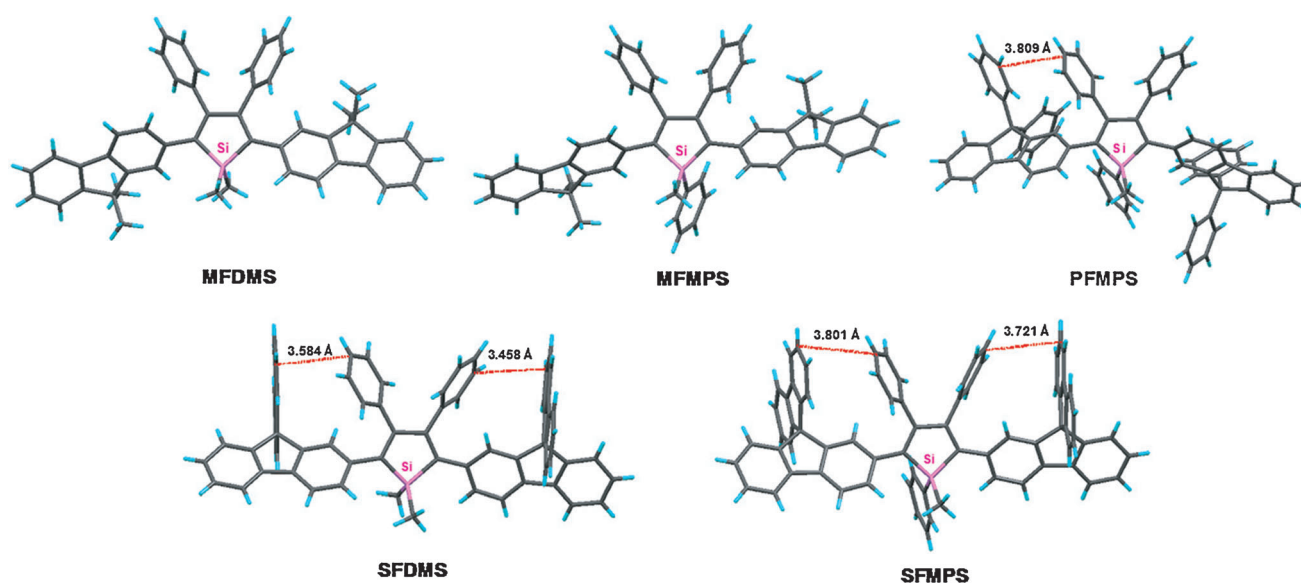


Figure 2. Crystal structures of MFDMS, MFMPs, PFMPs, SFDMS, and SFMPs, with indicated distances between aromatic rings.

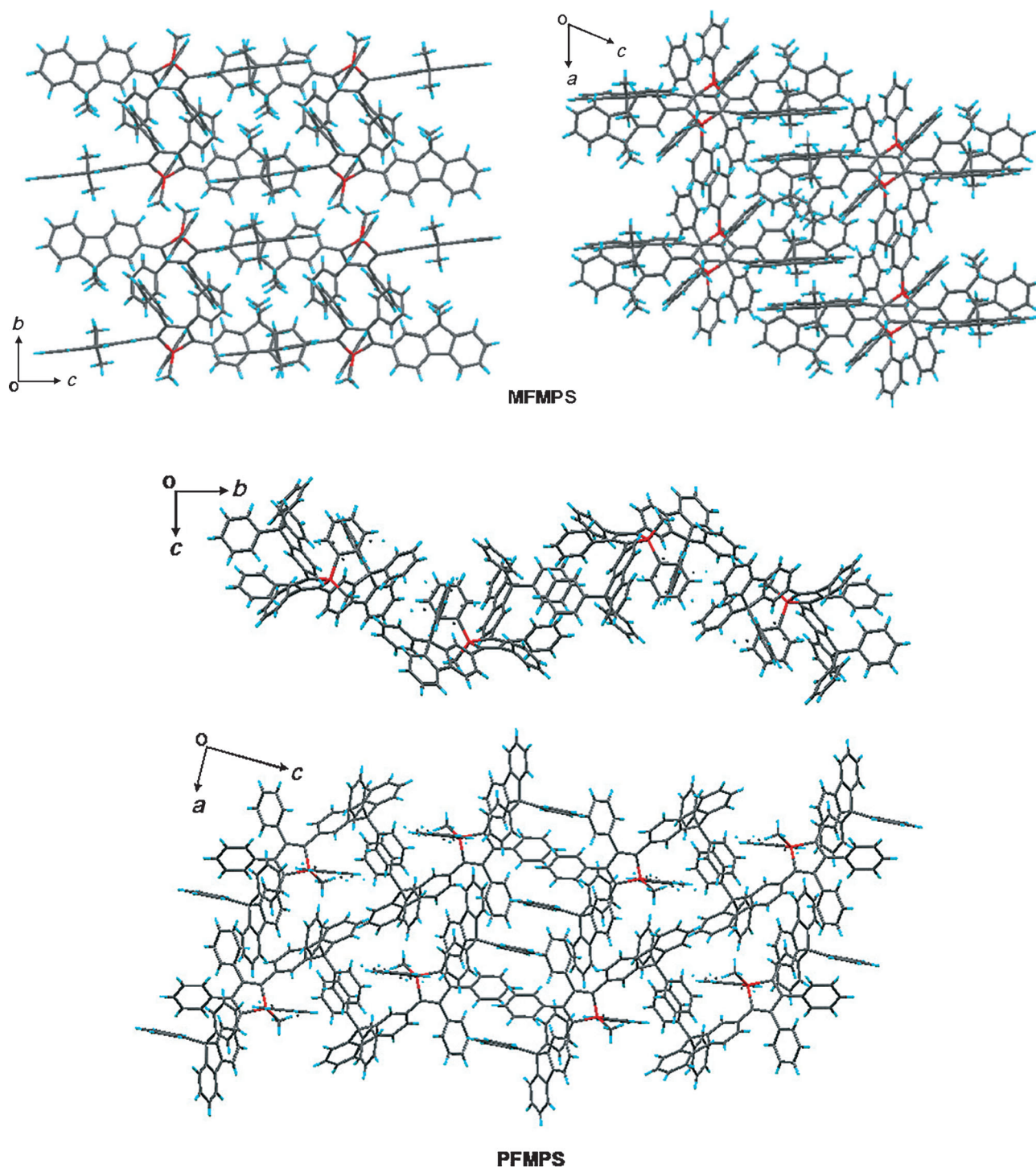


Figure 3. Molecular packing of MFMPs and PFMPs in the crystal.

The PL properties of the siloles were further investigated in the aggregated state. For example, Figure 5 shows the PL spectra of MFMPs and SFMPs in THF/water mixtures. On addition of water to their THF solutions, the blue emission bands weakened gradually and then disappeared. Meanwhile, the long-wavelength emission bands intensified swiftly and became dominant with slight redshifts (Table 1) when a large amount of water is added. Since water is a nonsolvent for MFMPs and SFMPs, their molecules must have aggregated in THF/water

mixtures with large fractions of water. The emission enhancement in the aggregated state relative to the molecularly dispersed state is indicative of aggregation-enhanced emission (AEE) characteristics. Similar emission behaviors were also found for the other 2,5-difluorenyl-substituted siloles. In the aggregated state, restricted intramolecular rotation promotes radiative decay of the excited state and allows the molecules to fluoresce intensely. The restriction of intramolecular rotation also augments the molecular conjugation and facilitates syner-

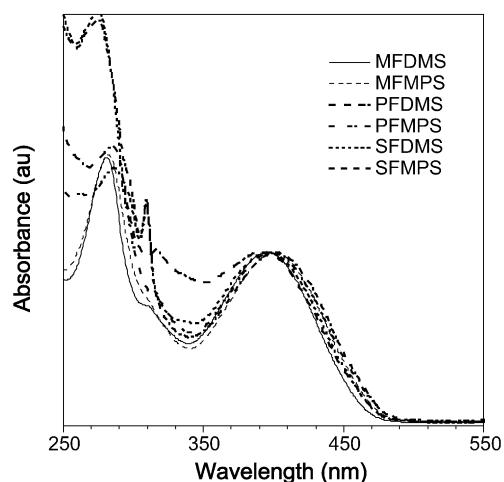


Figure 4. Absorption spectra of 2,5-difluorenyl-substituted siloles in THF solution.

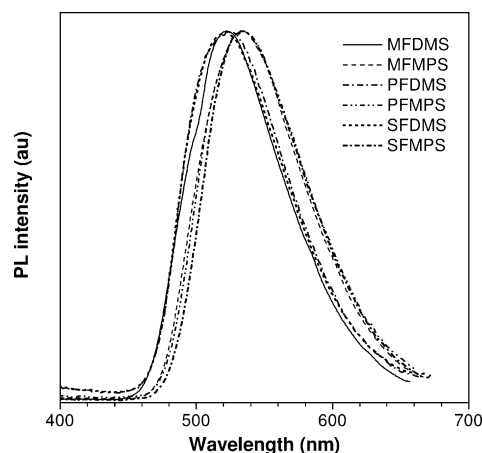


Figure 6. Photoluminescence spectra of the solid films of 2,5-difluorenyl-substituted siloles, excited at 350 nm.

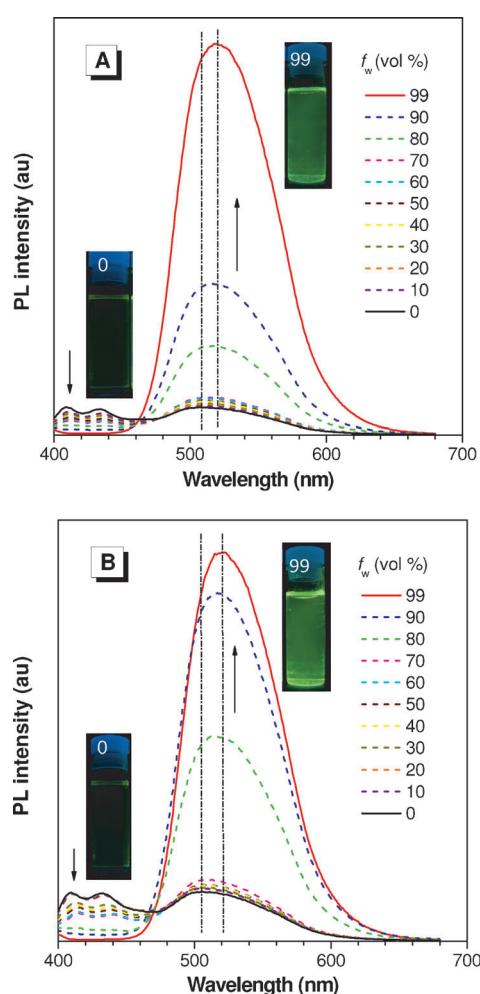


Figure 5. Photoluminescence spectra of A) MFMPs and B) SFMPs in THF/water with different water fractions f_w , excited at 350 nm. Inset: photographs of A) MFMPs and B) SFMPs in THF/water ($f_w=0$ and 99%) under illumination with a UV lamp.

getic effects between the neighboring segments. Eventually, the blue emission bands of fluorenyl substituents vanish and the PL spectra are dominated by the slightly redshifted and

enhanced long-wavelength emissions from the entire conjugated backbone comprising the silole ring and the two fluorenyl substituents.

The new siloles are highly emissive in the solid state. The PL spectra of their films are displayed in Figure 6. The film of MFMPs emits at 534 nm, which is slightly redshifted relative to MFDMS (523 nm). The films of other siloles exhibit comparable PL emissions peaking in the range of 521–535 nm. Their high Φ_F values of 75–88%, which were estimated from their solid films by integrating sphere, are improved greatly compared with those in solution. This further confirms that they are AEE-active and are potential light-emitting materials for undoped OLEDs.

Electroluminescence properties

To systematically evaluate the electroluminescence (EL) properties of the siloles, multilayer OLEDs with a configuration of indium tin oxide (ITO)/NPB (60 nm)/emitter (20 nm)/TPBi (40 nm)/LiF (1 nm)/Al (100 nm) were fabricated, in which the 2,5-difluorenyl-substituted siloles acted as light-emitting layers, *N,N*-bis(1-naphthyl)-*N,N*-diphenylbenzidine (NPB) as a hole-transporting layer, and 1,3,5-tris(*N*-phenylbenzimidazole-2-yl)-benzene (TPBi) as an electron-transporting layer. Table 2 lists the device performance data and CIE chromaticity coordinates, and Figure 7 displays the EL spectra and characteristic curves of the devices. MFDMS shows green EL emission at 520 nm (CIE 0.31, 0.57), and MFMPs exhibits yellow light at 544 nm (CIE 0.37, 0.57). Similar redshifts are also observed between the EL peaks of PFDMS (548 nm) and PFMPs (556 nm), as well as between those of SFDMS (524 nm) and SFMPs (540 nm). All the devices can be turned on at low voltages (3.2–4.4 V) and perform efficiently. The MFMPs-based device shows the lowest turn-on voltage of 3.2 V, but the highest maximum luminance L_{\max} of 31900 cd m^{-2} . The maximum current efficiency $\eta_{C,\max}$, maximum power efficiency $\eta_{P,\max}$ and maximum external quantum efficiency $\eta_{\text{ext},\max}$ attained by the device are as high as 16.0 cd A^{-1} , 13.5 lm W^{-1} , and 4.8%, respectively. The MFDMS-based device also shows good performance with $L_{\max} =$

	CIE	V_{on} [V]	L_{max} [$cd\ m^{-2}$]	$\eta_{C,max}$ [$cd\ A^{-1}$]	$\eta_{P,max}$ [$lm\ W^{-1}$]	$\eta_{ext,max}$ [%]
MFDMS	0.31, 0.57	3.2	27 600	12.9	11.6	4.0
MFMPs	0.37, 0.57	3.2	31 900	16.0	13.5	4.8
PFDMS	0.39, 0.53	4.4	8120	9.0	5.2	2.9
PFMPs	0.43, 0.52	4.4	7920	10.1	6.4	3.3
SFDMS	0.32, 0.57	3.8	10 400	9.1	6.9	2.8
SFMPs	0.35, 0.57	3.6	17 000	12.4	9.9	3.7

[a] Device configuration: ITO/NPB (60 nm)/emitter (20 nm)/TPBi (40 nm)/LiF (1 nm)/Al (100 nm). V_{on} =turn-on voltage at $1\ cd\ m^{-2}$; L_{max} =maximum luminance; $\eta_{P,max}$, $\eta_{C,max}$ and $\eta_{ext,max}$ =maximum power, current, and external quantum efficiency, respectively.

27 600 $cd\ m^{-2}$, $\eta_{C,max}=12.9\ cd\ A^{-1}$, $\eta_{P,max}=11.6\ cd\ A^{-1}$, and $\eta_{ext,max}=4.0\ %$. The devices based on PFDMS, PFMPs, SFDMS, and SFMPs, which bear more bulky substituents at the 2,5-positions, exhibit slightly decreased performances, but the efficiencies (9.0–12.4 $cd\ A^{-1}$, 5.2–9.9 $lm\ W^{-1}$, and 2.9–3.7%) are still much higher than those of most silole derivatives in the literature.^[12] The substituents at the 1,1-positions of silole ring have an obvious impact on the EL property of the siloles. Siloles with one phenyl ring and one methyl group at the 1,1-positions outperform analogues with two methyl groups (Table 2).

To further improve the EL performances, the device structure was optimized. To this end, MFMPs was selected as light emitter, because it showed the best EL properties in the above standard devices. An electrochemical study revealed that the film of MFMPs has a LUMO energy level of $-2.8\ eV$, which is slightly lower than that of TPBi ($-2.7\ eV$), and its HOMO energy level ($-5.4\ eV$) is equal to that of NPB. The matched LUMO energy levels between MFMPs and TPBi and HOMO energy levels between MFMPs and NPB should facilitate electron and hole injection into the MFMPs layer, and hence exciton generation. Therefore, NPB and TPBi were chosen as hole- and electron-transporting layers, respectively. The thickness of TPBi was increased from 20 to 60 nm to achieve a good balance between holes and electrons. In addition, a thin layer of

MoO₃ was added to facilitate hole injection. Multilayer devices with a configuration of ITO/MoO₃ (5 nm)/NPB (60 nm)/MFMPs (20 nm)/TPBi ($x\ nm$)/LiF (1 nm)/Al (100 nm) (device A, $x=20$; device B, $x=30$; device C, $x=40$; device D, $x=60$) were fabricated. The MFMPs-based devices exhibit stable emission of yellow light with only slight differences in their EL spectra (Figure 8A). The EL spectra are similar to the PL spectrum of MFMPs in the film indicating that the EL emission originates from radiative decay of the excited singlet state. The EL efficiencies of the devices improved gradually on increasing the thickness of the TPBi layer (Figure 8B) and reached a maximum in device D. The current densities at identical voltages, however, decreased. The TPBi layer should function as a hole blocker in addition to acting as an electron transporter. With increasing thickness of TPBi, more holes and electrons are confined in the light-emitting layer, and this results in a high recombination efficiency of excitons and thus high power efficiency (Table 3). The most efficient device D is turned on at 3.3 V and emitted intense yellow light (CIE 0.36, 0.57) with an L_{max} value of 37 800 $cd\ m^{-2}$ and remarkably high $\eta_{C,max}$ value of 18.3 $cd\ A^{-1}$ and $\eta_{P,max}$ value of 15.7 $lm\ W^{-1}$. Significantly, an impressive $\eta_{ext,max}$ value of 5.5% was achieved. Since MFMPs contains no heavy-metal atoms, triplet-to-singlet energy conversion is negligible. Thus, an unusually high singlet-triplet branching ratio ($>1:3$) is probably responsible for such a high $\eta_{ext,max}$ value, which had been demonstrated to be possible in conjugated polymers^[18] as well as other siloles.^[9a] Thus, a new breakthrough in EL efficiency may be achieved by judicious molecular engineering and device optimization.

Conclusion

A series of silole derivatives with different-sized fluorenyl substituents were synthesized and fully characterized. The presence of bulky aromatic substituents causes spatial congestion which partially suppresses intramolecular rotation. Therefore, these new siloles show higher emission efficiencies than 2,3,4,5-tetraphenylsiloles in solution. In the aggregated state, the intramolecular rotation is further restricted, and they

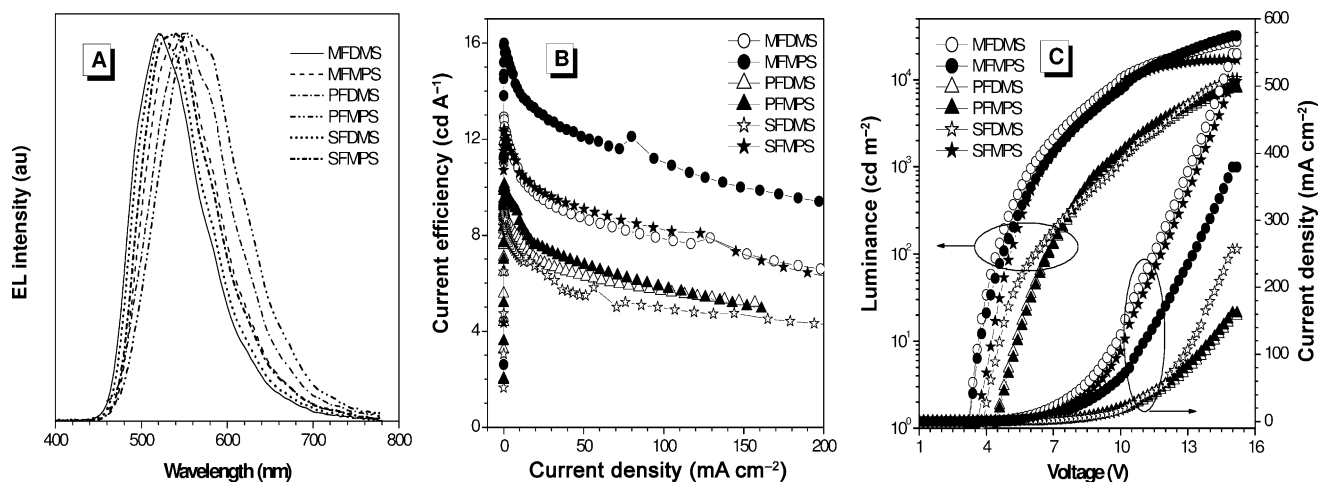


Figure 7. A) Electroluminescence spectra of 2,5-bifluorenyl-substituted siloles, B) plots of current efficiency versus current density, and C) changes in luminance and current density with applied voltage in multilayer devices with a configuration of ITO/NPB (60 nm)/emitter (20 nm)/TPBi (40 nm)/LiF (1 nm)/Al (100 nm).

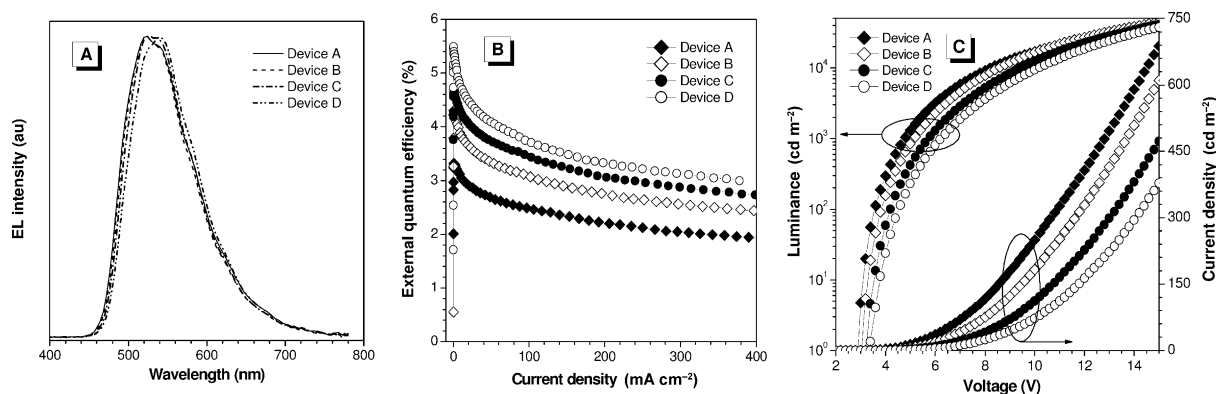


Figure 8. A) Electroluminescence spectra, B) plots of external quantum efficiency versus current density, and C) changes in luminance and current density with the applied voltage in multilayer devices with configurations of ITO/MoO₃ (5 nm)/NPB (60 nm)/MFMPs (20 nm)/TPBi (x nm)/LiF (1 nm)/Al (100 nm) (device A, x = 20; device B, x = 30; device C, x = 40; device D, x = 60).

Device	CIE	V _{on} [V]	L _{max} [cd m ⁻²]	η _{C,max} [cd A ⁻¹]	η _{P,max} [lm W ⁻¹]	η _{ext,max} [%]
A	0.34, 0.56	2.9	37 500	10.7	10.2	3.3
B	0.34, 0.57	3.1	44 100	14.0	12.7	4.3
C	0.34, 0.57	3.2	41 100	15.4	12.8	4.7
D	0.36, 0.57	3.3	37 800	18.3	15.7	5.5

[a] Device configuration: ITO/MoO₃ (5 nm)/NPB (60 nm)/MFMPs (20 nm)/TPBi (x nm)/LiF (1 nm)/Al (100 nm) (device A, x = 20; device B, x = 30; device C, x = 40; device D, x = 60). V_{on} = turn-on voltage at 1 cd m⁻²; L_{max} = maximum luminance; η_{P,max}, η_{C,max} and η_{ext,max} = maximum power, current, and external quantum efficiency, respectively.

become highly emissive with Φ_F values of 75–86%. Thus, incorporation of bulky substituents converts siloles to AEE luminogens. The phenyl ring at the 1-position of the silole ring also affects the photophysical properties of siloles, such as redshifted absorption and emission spectra. The applications of these new siloles were investigated. Multilayer devices fabricated with silole host emitters show outstanding performance, and thus they are promising light emitters for OLEDs. It is noteworthy that siloles with one phenyl ring and one methyl group can function better than those with two methyl groups at the 1,1-positions. In particular, an optimized MFMPs-based device is one of the most efficient OLEDs based on siloles, and gives remarkably high EL efficiencies of 18.3 cd A⁻¹, 15.7 lm W⁻¹, and 5.5%.

Experimental Section

Materials and instruments

THF was distilled from sodium benzophenone ketyl under dry nitrogen immediately prior to use. All other chemicals and reagents were purchased from J&K Scientific Ltd. and used as received without further purification. ¹H and ¹³C NMR spectra were measured on a Bruker AV 400 spectrometer in deuterated chloroform with TMS ($\delta=0$) as internal reference. UV spectra were measured on a Milton Roy Spectronic 3000 Array spectrophotometer. PL spectra were recorded on a PerkinElmer LS 55 spectrofluorometer. High-resolution mass spectra (HRMS) were recorded on a GCT premier CAB048 mass spectrometer operating in MALDI-TOF mode. Ele-

mental analysis was performed on an Elementary Vario EL analyzer. Single-crystal X-ray diffraction intensity data were collected at 100 K on a Bruker Nonius Smart Apex CCD diffractometer with graphite-monochromated MoK α radiation. The intensity data were processed by using the SAINT and SADABS routines, and the structure solution and refinement were conducted with the SHELTL suite of X-ray programs (version 6.10). TGA analysis was carried on a TA TGA Q5000 under dry nitrogen at a heating rate of 10 °C min⁻¹. The ground-state geometries were optimized DFT with B3LYP hybrid functional and 6-31G(d) basis set. All calculations were performed with the Gaussian 09 package.

Device fabrication

The devices were fabricated on glass with 80 nm ITO coating having a sheet resistance of 25 Ω sq⁻¹. Prior to loading into the pretreatment chamber, the ITO-coated glass was soaked in ultrasonic detergent for 30 min, followed by spraying with deionized water for 10 min, soaking in ultrasonic deionized water for 30 min, and oven-baking for 1 h. The cleaned samples were treated with a tetrafluoromethane plasma with a power of 100 W, a gas flow of 50 sccm, and a pressure of 0.2 Torr for 10 s in the pretreatment chamber. The samples were transferred to the organic chamber with a base pressure of 7×10^{-7} Torr for the deposition of NPB, emitter, and TPBi, which served as hole-transport, light-emitting, and electron-transport layers, respectively. The samples were then transferred to the metal chamber for deposition of a cathode composed of LiF capped with Al. The light-emitting area was 4 mm². The current density/voltage characteristics of the devices were measured by a HP4145B semiconductor parameter analyzer. The forward-direction photons emitted from the devices were detected by a calibrated UDT PIN-25D silicon photodiode. The luminance and external quantum efficiencies of the devices were inferred from the photocurrent of the photodiode. The electroluminescence spectra were obtained by a PR650 spectrophotometer. All measurements were carried out under air at room temperature without device encapsulation.

Synthesis

2,5-Bis(9,9-dimethylfluoren-2-yl)-1,1-dimethyl-3,4-diphenylsilole (MFDMS): A solution of lithium naphthalenide (LiNaph) was prepared by stirring a mixture of naphthalene (1.28 g, 10 mmol) and lithium granules (0.07 g, 10 mmol) in dry THF (30 mL) for 4 h at room temperature under nitrogen. A solution of bis(phenylethynyl)dimethylsilane (**1a**; 0.65 g, 2.5 mmol) in THF (20 mL) was then

added dropwise to the solution of LiNaph, and the resultant mixture was stirred for 1 h at room temperature. After the solution was cooled to -10°C , $\text{ZnCl}_2\cdot\text{TMEDA}$ (3.2 g, 12.5 mmol) and 20 mL of THF were added. The fine suspension was stirred for 1 h at room temperature and $[\text{Pd}(\text{PPh}_3)_2\text{Cl}_2]$ (105 mg, 0.15 mmol), 2-bromo-9,9-dimethylfluorene (1.7 g, 6.3 mmol), and 10 mL of THF were then added. After heating to reflux for 12 h, the reaction mixture was cooled to room temperature and the reaction terminated by addition of 1 M hydrochloric acid. The mixture was poured into water and extracted with dichloromethane. The organic layer was washed successively with saturated brine and water, and dried over magnesium sulfate. After filtration, the solvent was evaporated under reduced pressure and the residue was purified by silica-gel column chromatography with *n*-hexane/dichloromethane as eluent. MFDMS was obtained as a bright yellow solid in 58% yield based on **1a**. $^1\text{H NMR}$ (400 MHz, CDCl_3): $\delta = 7.66$ (d, 2H, $J = 7.6$ Hz), 7.57 (d, 2H, $J = 8.0$ Hz), 7.36 (d, 2H, $J = 7.6$ Hz), 7.32–7.24 (m, 4H), 7.13 (dd, 2H, $J_1 = 7.6$ Hz, $J_2 = 1.6$ Hz), 7.06–7.04 (m, 6H), 6.92–6.90 (m, 4H), 6.81 (s, 2H), 1.22 (s, 12H), 0.62 ppm (s, 6H); $^{13}\text{C NMR}$ (100 MHz, CDCl_3): $\delta = 154.1$, 153.9, 153.1, 141.7, 139.4, 139.2, 138.9, 136.7, 130.1, 128.0, 127.6, 126.8, 126.2, 123.4, 122.5, 119.7, 119.4, 46.3, 26.9, -3.1 ppm; HRMS (MALDI-TOF): m/z calcd: 646.3056; found: 646.3064 $[\text{M}]^+$; elemental analysis (%) calcd for $\text{C}_{48}\text{H}_{42}\text{Si}$: C 89.11, H 6.54; found: C 89.02, H 6.43.

2,5-Bis(9,9-dimethylfluorene-2-yl)-1-methyl-1,3,4-triphenylsilole (MFMPs): The procedure was analogous to that described for MFDMS. Bright yellow solid, yield 50%. $^1\text{H NMR}$ (400 MHz, CDCl_3): $\delta = 7.75$ (d, 2H, $J = 5.6$ Hz), 7.56 (d, 2H, $J = 7.6$ Hz), 7.43–7.37 (m, 5H), 7.31 (d, 2H, $J = 6.8$ Hz), 7.26–7.19 (m, 4H), 7.07 (br, 6H), 6.99–6.95 (m, 6H), 6.77 (s, 2H), 1.13 (s, 12H), 0.91 ppm (s, 3H); $^{13}\text{C NMR}$ (100 MHz, CDCl_3): $\delta = 155.6$, 153.8, 153.0, 140.4, 139.5, 139.1, 138.4, 136.8, 134.8, 134.2, 130.0, 129.9, 128.3, 128.2, 127.8, 126.8, 126.4, 123.6, 122.5, 119.8, 119.4, 46.3, 26.9, 26.8, -5.7 ppm; HRMS (MALDI-TOF): m/z calcd: 708.3212; found: 708.3255 $[\text{M}]^+$; elemental analysis (%) calcd for $\text{C}_{53}\text{H}_{44}\text{Si}$: C 89.78, H 6.26; found: C 89.67, H 6.21.

2,5-Bis(9,9-diphenylfluorene-2-yl)-1,1-dimethyl-3,4-diphenylsilole (PFDMS): The procedure was analogous to that described for MFDMS. Greenish-yellow solid, yield 44%. $^1\text{H NMR}$ (400 MHz, CDCl_3): $\delta = 7.64$ (d, 2H, $J = 8.0$ Hz), 7.53 (d, 2H, $J = 7.6$ Hz), 7.35 (d, 2H, $J = 7.6$ Hz), 7.31–7.27 (m, 2H), 7.22–7.12 (m, 14H), 7.01–6.91 (m, 18H), 6.79–6.77 (m, 4H), 0.33 ppm (s, 6H); $^{13}\text{C NMR}$ (100 MHz, CDCl_3): $\delta = 154.0$, 151.1, 150.8, 146.0, 141.7, 140.1, 139.3, 139.0, 137.7, 129.7, 128.3, 128.0, 127.5, 127.4, 127.3, 126.9, 126.3, 126.1, 119.9, 119.7, 65.2, -3.6 ppm; HRMS (MALDI-TOF): m/z calcd: 894.3682; found: 894.3685 $[\text{M}]^+$; elemental analysis (%) calcd for $\text{C}_{68}\text{H}_{50}\text{Si}$: C 91.23, H 5.63; found: C 91.12, H 5.61.

2,5-Bis(9,9-diphenylfluorene-2-yl)-1-methyl-1,3,4-triphenylsilole (PFMPs): The procedure was analogous to that described for MFDMS. Greenish-yellow solid, yield 26%. $^1\text{H NMR}$ (400 MHz, CDCl_3): $\delta = 7.59$ (d, 2H, $J = 7.6$ Hz), 7.45–7.42 (m, 4H), 7.36–7.32 (m, 3H), 7.28–7.25 (m, 2H), 7.20–7.12 (m, 12H), 7.10–7.06 (m, 4H), 6.96–6.94 (m, 12H), 6.89–6.88 (m, 6H), 6.85–6.83 (m, 4H), 0.69 ppm (s, 3H); $^{13}\text{C NMR}$ (100 MHz, CDCl_3): $\delta = 155.4$, 151.1, 150.7, 146.1, 145.7, 140.5, 140.1, 138.9, 137.7, 134.6, 133.7, 129.8, 129.6, 128.5, 128.1, 128.0, 127.6, 127.3, 127.2, 126.5, 126.3, 126.2, 126.1, 119.9, 119.6, 65.2, -6.1 ppm; HRMS (MALDI-TOF): m/z calcd: 956.3838; found: 956.3847 $[\text{M}]^+$; elemental analysis (%) calcd for $\text{C}_{73}\text{H}_{52}\text{Si}$: C 91.59, H 5.48; found: C 91.62, H 5.32.

2,5-Bis(9,9'-spirobifluorene-2-yl)-1,1-dimethyl-3,4-diphenylsilole (SFDMS): The procedure was analogous to that described for MFDMS. Yellow solid, yield 45%. $^1\text{H NMR}$ (400 MHz, CDCl_3): $\delta = 7.72$ –7.69 (m, 6H), 7.60 (d, 2H, $J = 8.0$ Hz), 7.30–7.26 (m, 6H), 7.05–

6.99 (m, 8H), 6.65–6.55 (m, 12H), 6.46–6.43 (m, 4H), 5.94 (d, 2H, $J = 1.2$ Hz), 0.22 ppm (s, 6H); $^{13}\text{C NMR}$ (100 MHz, CDCl_3): $\delta = 154.8$, 149.6, 149.3, 149.1, 142.4, 142.2, 141.7, 140.1, 139.8, 139.0, 129.9, 129.2, 128.3, 128.2, 127.7, 126.9, 125.3, 124.6, 120.4, 120.3, 120.0, 66.3, -2.9 ppm; HRMS (MALDI-TOF): m/z calcd: 890.3369; found: 890.3336 $[\text{M}]^+$; elemental analysis (%) calcd for $\text{C}_{68}\text{H}_{46}\text{Si}$: C 91.65, H 5.20; found: C 91.53, H 5.12.

2,5-Bis(9,9'-spirobifluorene-2-yl)-1-methyl-1,3,4-triphenylsilole (SFMPs): The procedure was analogous to that described for MFDMS. Yellow solid, yield 22%. $^1\text{H NMR}$ (400 MHz, CDCl_3): $\delta = 7.75$ (d, 2H, $J = 8.0$ Hz), 7.72 (d, 2H, $J = 7.6$ Hz), 7.66 (d, 2H, $J = 7.2$ Hz), 7.48 (d, 2H, $J = 8.0$ Hz), 7.35–7.21 (m, 8H), 7.11–6.99 (m, 9H), 6.87 (dd, 2H, $J_1 = 8.0$ Hz, $J_2 = 1.6$ Hz), 6.75–6.67 (m, 6H), 6.62 (d, 2H, $J = 7.2$ Hz), 6.58–6.54 (m, 8H), 6.03 (d, 2H, $J = 1.6$ Hz), 0.49 ppm (s, 3H); $^{13}\text{C NMR}$ (100 MHz, CDCl_3): $\delta = 156.1$, 149.5, 149.4, 149.2, 149.1, 142.4, 142.2, 140.6, 139.8, 139.7, 139.1, 135.2, 134.3, 130.1, 130.0, 129.3, 128.6, 128.2, 128.0, 127.8, 127.0, 125.5, 124.6, 124.5, 120.4, 120.3, 120.0, 66.3, -5.3 ppm; HRMS (MALDI-TOF): m/z calcd: 952.3525; found: 952.2321 $[\text{M}]^+$; elemental analysis (%) calcd for $\text{C}_{73}\text{H}_{48}\text{Si}$: C 91.98, H 5.08; found: C 91.88, H 5.11.

X-ray crystallography

Crystal data for MFDMS: $\text{C}_{48}\text{H}_{42}\text{Si}$, $M = 646.91$, monoclinic, $P2_1/c$; $a = 14.9064(3)$, $b = 14.8156(3)$, $c = 16.8849(3)$ Å; $\beta = 93.800(2)^{\circ}$; $V = 2080.31(19)$ Å³; $Z = 4$; $\rho_{\text{calcd}} = 1.155$ g cm⁻³; $\mu = 0.786$ mm⁻¹ ($\text{Mo}_{\text{K}\alpha}$ $\lambda = 1.5418$); $F(000) = 1376$; $T = 173.00(14)$ K; $2\theta_{\text{max}} = 66.5^{\circ}$; 20913 measured reflections, 6519 independent reflections ($R_{\text{int}} = 0.0371$); GOF on $F^2 = 1.002$, $R_1 = 0.0415$, $wR_2 = 0.0953$ (all data); $\Delta\rho_{\text{max}}/\Delta\rho_{\text{min}} = 0.253/-0.204$ e Å⁻³.

Crystal data for MFMPs: $\text{C}_{53}\text{H}_{44}\text{Si}$, $M = 708.97$, triclinic, $P\bar{1}$; $a = 11.6363(4)$, $b = 13.6358(8)$, $c = 14.3392(5)$ Å; $\alpha = 86.769(4)$, $\beta = 69.216(3)$, $\gamma = 71.632(4)^{\circ}$; $V = 2014.83(15)$ Å³; $Z = 2$; $\rho_{\text{calcd}} = 1.169$ g cm⁻³; $\mu = 0.771$ mm⁻¹ ($\text{Mo}_{\text{K}\alpha}$ $\lambda = 1.5418$); $F(000) = 752$; $T = 173.00(14)$ K; $2\theta_{\text{max}} = 66.5^{\circ}$; 10982 measured reflections, 6646 independent reflections ($R_{\text{int}} = 0.0440$); GOF on $F^2 = 1.006$, $R_1 = 0.0665$, $wR_2 = 0.1601$ (all data); $\Delta\rho_{\text{max}}/\Delta\rho_{\text{min}} = 0.889/-0.440$ e Å⁻³.

Crystal data for PFMPs: $\text{C}_{73}\text{H}_{52}\text{Si}$, $M = 957.24$, monoclinic, $P2_1/c$; $a = 10.6497(4)$, $b = 10.5425(4)$, $c = 47.000(2)$ Å; $\beta = 93.176(4)^{\circ}$; $V = 5268.8(4)$ Å³; $Z = 4$; $\rho_{\text{calcd}} = 1.207$ g cm⁻³; $\mu = 0.726$ mm⁻¹ ($\text{Mo}_{\text{K}\alpha}$ $\lambda = 1.5418$); $F(000) = 2016$; $T = 173.00(14)$ K; $2\theta_{\text{max}} = 66.5^{\circ}$; 28304 measured reflections, 9269 independent reflections ($R_{\text{int}} = 0.0430$); GOF on $F^2 = 1.005$, $R_1 = 0.0596$, $wR_2 = 0.1289$ (all data); $\Delta\rho_{\text{max}}/\Delta\rho_{\text{min}} = 0.333/-0.388$ e Å⁻³.

Crystal data for SFDMS: $\text{C}_{68}\text{H}_{46}\text{Si}\cdot 4\text{CH}_2\text{Cl}_2$, $M = 1230.84$, monoclinic, $P2_1/n$; $a = 17.1363(14)$, $b = 13.2945(17)$, $c = 27.0677(14)$ Å; $\beta = 97.761(10)^{\circ}$; $V = 6110.0(10)$ Å³; $Z = 4$; $\rho_{\text{calcd}} = 1.338$ g cm⁻³; $\mu = 0.432$ mm⁻¹ ($\text{Mo}_{\text{K}\alpha}$ $\lambda = 0.71073$); $F(000) = 2544$; $T = 291(2)$ K; $2\theta_{\text{max}} = 25.242^{\circ}$; 26063 measured reflections, 11140 independent reflections ($R_{\text{int}} = 0.0142$); GOF on $F^2 = 1.047$, $R_1 = 0.0674$, $wR_2 = 0.1216$ (all data); $\Delta\rho_{\text{max}}/\Delta\rho_{\text{min}} = 0.580/-0.366$ e Å⁻³.

Crystal data for SFMPs: $\text{C}_{73}\text{H}_{48}\text{Si}\cdot 4\text{CH}_2\text{Cl}_2$, $M = 1292.90$, monoclinic, $P2_1/c$; $a = 16.0520(12)$, $b = 10.498(2)$, $c = 39.5040(19)$ Å; $\beta = 92.88(3)^{\circ}$; $V = 6648.6(15)$ Å³; $Z = 4$; $\rho_{\text{calcd}} = 1.292$ g cm⁻³; $\mu = 0.400$ mm⁻¹ ($\text{Mo}_{\text{K}\alpha}$ $\lambda = 0.71073$); $F(000) = 2672$; $T = 291(2)$ K; $2\theta_{\text{max}} = 25.242^{\circ}$; 40718 measured reflections, 12774 independent reflections ($R_{\text{int}} = 0.0159$); GOF on $F^2 = 1.062$, $R_1 = 0.0622$, $wR_2 = 0.1563$ (all data); $\Delta\rho_{\text{max}}/\Delta\rho_{\text{min}} = 0.950/-0.505$ e Å⁻³.

CCDC-928433 (MFDMS), CCDC-928434 (MFMPs), CCDC-928435 (PFMPs), CCDC-951834 (SFDMS) and CCDC-951835 (SFMPs) contain the supplementary crystallographic data for this paper. These data can be obtained free of charge from The Cambridge Crystallographic Data Centre via www.ccdc.cam.ac.uk/data_request/cif.

Acknowledgements

We acknowledge the financial support from the National Natural Science Foundation of China (51273053 and 21104012), the National Basic Research Program of China (973 Program, 2013CB834702), the Fundamental Research Funds for the Central Universities (2013ZZ0002), and the Program for Changjiang Scholars and Innovative Research Teams in Chinese Universities (IRT 1231). B.Z.T. thanks the support of the Guangdong Innovative Research Team Program of China (20110C0105067115) and the Research Grants Council of Hong Kong (HKUST2/CRF/10).

Keywords: aggregation · luminescence · organic light-emitting diodes · siloles · steric hindrance

- [1] a) J. Luo, Z. Xie, J. W. Y. Lam, L. Cheng, H. Chen, C. Qiu, H. S. Kwok, X. Zhan, Y. Liu, D. Zhu, B. Z. Tang, *Chem. Commun.* **2001**, 1740; b) J. Chen, C. C. W. Law, J. W. Y. Lam, Y. Dong, S. M. F. Lo, I. D. Williams, D. Zhu, B. Z. Tang, *Chem. Mater.* **2003**, *15*, 1535; c) Z. Zhao, Z. Wang, P. Lu, C. Y. K. Chan, D. Liu, J. W. Y. Lam, H. H. Y. Sung, I. D. Williams, Y. Ma, B. Z. Tang, *Angew. Chem.* **2009**, *121*, 7744; *Angew. Chem. Int. Ed.* **2009**, *48*, 7608; d) Z. Li, Y. Dong, J. W. Y. Lam, J. Sun, A. Qin, M. Häußler, Y. Dong, H. H. Y. Sung, I. D. Williams, H. S. Kwok, B. Z. Tang, *Adv. Funct. Mater.* **2009**, *19*, 905; e) J. Zhou, B. He, B. Chen, P. Lu, H. H. Y. Sung, I. D. Williams, A. Qin, H. Qiu, Z. Zhao, B. Z. Tang, *Dyes Pigm.* **2013**, *99*, 520; f) Y. Yabusaki, N. Ohshima, H. Kondo, T. Kusamoto, Y. Yamanoi, H. Nishihara, *Chem. Eur. J.* **2010**, *16*, 5581.
- [2] a) B.-K. An, S.-K. Kwon, S.-D. Jung, S. Y. Park, *J. Am. Chem. Soc.* **2002**, *124*, 14410; b) B.-K. An, D.-S. Lee, J.-S. Lee, Y.-S. Park, H.-S. Song, S. Y. Park, *J. Am. Chem. Soc.* **2004**, *126*, 10232; c) B.-K. An, J. Gierschner, S. Y. Park, *Acc. Chem. Res.* **2012**, *45*, 544.
- [3] a) Z. Zhao, J. W. Y. Lam, B. Z. Tang, *Curr. Org. Chem.* **2010**, *14*, 2109; b) Z. Zhao, S. Chen, X. Shen, F. Mahtab, Y. Yu, P. Lu, J. W. Y. Lam, H. S. Kwok, B. Z. Tang, *Chem. Commun.* **2010**, 46, 686; c) Y. Dong, J. W. Y. Lam, A. Qin, J. Liu, Z. Li, B. Z. Tang, J. Sun, H. S. Kwok, *Appl. Phys. Lett.* **2007**, *91*, 011111.
- [4] a) H. Tong, Y. Dong, Y. Hong, M. Häußler, J. W. Y. Lam, H. H.-Y. Sung, X. Yu, J. Sun, I. D. Williams, H. S. Kwok, B. Z. Tang, *J. Phys. Chem. C* **2007**, *111*, 2287; b) Y. Dong, J. W. Y. Lam, A. Qin, Z. Li, J. Sun, H. H. Y. Sung, I. D. Williams, B. Z. Tang, *Chem. Commun.* **2007**, 40; c) X. Luo, J. Li, C. Li, L. Heng, Y. Dong, Z. Liu, Z. Bo, B. Z. Tang, *Adv. Mater.* **2011**, *23*, 3261.
- [5] a) K. Shiraishi, T. Kashiwabara, T. Sanji, M. Tanaka, *New J. Chem.* **2009**, *33*, 1680; b) T. Sanji, K. Shiraishi, M. Tanaka, *ACS Appl. Mater. Interfaces* **2009**, *1*, 270.
- [6] a) Z. Zhao, J. W. Y. Lam, B. Z. Tang, *J. Mater. Chem.* **2012**, *22*, 23726; b) Z. Zhao, S. Chen, J. W. Y. Lam, P. Lu, Y. Zhong, K. S. Wong, H. S. Kwok, B. Z. Tang, *Chem. Commun.* **2010**, 46, 2221; c) Z. Zhao, P. Lu, J. W. Y. Lam, Z. Wang, C. Y. K. Chan, H. H. Y. Sung, I. D. Williams, Y. Ma, B. Z. Tang, *Chem. Sci.* **2011**, *2*, 672; d) Z. Zhao, S. Chen, C. Y. K. Chan, J. W. Y. Lam, C. K. W. Jim, P. Lu, Z. Chang, H. S. Kwok, H. Qiu, B. Z. Tang, *Chem. Asian J.* **2012**, *7*, 484; e) Z. Chang, Y. Jiang, B. He, J. Chen, Z. Yang, P. Lu, H. S. Kwok, Z. Zhao, H. Qiu, B. Z. Tang, *Chem. Commun.* **2013**, 49, 594; f) Z. Zhao, J. W. Y. Lam, C. Y. K. Chan, S. Chen, J. Liu, P. Lu, M. Rodriguez, J.-L. Maldonado, G. Ramos-Ortiz, H. H. Y. Sung, I. D. Williams, H. Su, K. S. Wong, Y. Ma, H. S. Kwok, H. Qiu, B. Z. Tang, *Adv. Mater.* **2011**, *23*, 5430.
- [7] a) J. Y. Kim, T. Yasuda, Y. S. Yang, C. Adachi, *Adv. Mater.* **2013**, *25*, 2666; b) H. Li, Z. Chi, X. Zhang, B. Xu, S. Liu, Y. Zhang, J. Xu, *Chem. Commun.* **2011**, 47, 11273; c) X. Du, J. Qi, Z. Zhang, D. Ma, Z. Y. Wang, *Chem. Mater.* **2012**, *24*, 2178; d) J. Huang, N. Sun, J. Yang, R. Tang, Q. Li, D. Ma, J. Qin, Z. Li, *J. Mater. Chem.* **2012**, *22*, 12001; e) J. Huang, N. Sun, Y. Dong, R. Tang, P. Lu, P. Cai, Q. Li, D. Ma, J. Qin, Z. Li, *Adv. Funct. Mater.* **2013**, *23*, 2329; f) J. Huang, X. Yang, X. Li, P. Chen, R. Tang, F. Li, P. Lu, Y. Ma, L. Wang, J. Qin, Q. Li, Z. Li, *Chem. Commun.* **2012**, 48, 9586; g) J. Huang, X. Yang, J. Wang, C. Zhong, L. Wang, J. Qin, Z. Li, *J. Mater. Chem.* **2012**, *22*, 2478.
- [8] a) Y. Hong, J. W. Y. Lam, B. Z. Tang, *Chem. Soc. Rev.* **2011**, *40*, 5361; b) Y. Hong, J. W. Y. Lam, B. Z. Tang, *Chem. Commun.* **2009**, 4332.
- [9] a) H. Y. Chen, J. W. Lam, J. D. Luo, Y. L. Ho, B. Z. Tang, D. Zhu, M. Wong, H. S. Kwok, *Appl. Phys. Lett.* **2002**, *81*, 574; b) Z. Zhao, S. Chen, J. W. Y. Lam, C. K. W. Jim, C. Y. K. Chan, Z. Wang, P. Lu, H. S. Kwok, Y. Ma, B. Z. Tang, *J. Phys. Chem. C* **2010**, *114*, 7963; c) T. Jiang, Y. Jiang, W. Qin, S. Chen, Y. Lu, J. W. Y. Lam, B. He, P. Lu, H. H. Y. Sung, I. D. Williams, H. S. Kwok, Z. Zhao, H. Qiu, B. Z. Tang, *J. Mater. Chem.* **2012**, *22*, 20266; d) J. Mei, J. Wang, J. Z. Sun, H. Zhao, W. Yuan, C. Deng, S. Chen, H. H. Y. Sung, P. Lu, A. Qin, H. S. Kwok, Y. Ma, I. D. Williams, B. Z. Tang, *Chem. Sci.* **2012**, *3*, 549.
- [10] a) J. Lee, Q.-D. Liu, D.-R. Bai, Y. Kang, Y. Tao, S. Wang, *Organometallics* **2004**, *23*, 6205; b) H.-J. Son, W.-S. Han, J.-Y. Chun, C.-J. Lee, J.-I. Han, J. Ko, S. O. Kang, *Organometallics* **2007**, *26*, 519; c) L. Aubouy, N. Huby, L. Hirsch, A. van der Lee, P. Gerbier, *New J. Chem.* **2009**, *33*, 1290; d) H. Murata, Z. H. Kafafi, M. Uchida, *Appl. Phys. Lett.* **2002**, *80*, 189; e) L. C. Palilis, H. Murata, M. Uchida, Z. H. Kafafi, *Org. Electron.* **2003**, *4*, 113; f) L. Aubouy, P. Gerbier, N. Huby, G. Wantz, L. Vignau, L. Hirsch, J.-M. Janot, *New J. Chem.* **2004**, *28*, 1086; g) J. Lee, Y.-Y. Yuan, Y. Kang, W.-L. Jia, Z.-H. Lu, S. Wang, *Adv. Funct. Mater.* **2006**, *16*, 681; h) Y. Wang, L. Hou, K. Yang, J. Chen, F. Wang, Y. Cao, *Macromol. Chem. Phys.* **2005**, *206*, 2190.
- [11] a) K. Tamao, M. Uchida, T. Izumizawa, K. Furukawa, S. Yamaguchi, *J. Am. Chem. Soc.* **1996**, *118*, 11974; b) Z. Zhao, D. Liu, F. Mahtab, L. Xin, Z. Shen, Y. Yu, C. Y. K. Chan, P. Lu, J. W. Y. Lam, H. H. Y. Sung, I. D. Williams, B. Yang, Y. Ma, B. Z. Tang, *Chem. Eur. J.* **2011**, *17*, 5998; c) H.-J. Son, W.-S. Han, K. R. Wee, S.-H. Lee, A.-R. Hwang, S. Kwon, D. W. Cho, I.-H. Suh, S. O. Kang, *J. Mater. Chem.* **2009**, *19*, 8964; d) C. Risko, G. P. Kushto, Z. H. Kafati, J. L. Brédas, *J. Chem. Phys.* **2004**, *121*, 9031; e) M. Uchida, T. Izumizawa, T. Nakano, S. Yamaguchi, K. Tamao, K. Furukawa, *Chem. Mater.* **2001**, *13*, 2680; f) X. Zhan, A. Haldi, C. Risko, C. K. Chan, W. Zhao, T. V. Timofeeva, A. Korlyukov, M. Y. Antipin, S. Montgomery, E. Thompson, Z. An, B. Domerq, S. Barlow, A. Kahn, B. Kippelen, J.-L. Brédas, S. R. Marder, *J. Mater. Chem.* **2008**, *18*, 3157.
- [12] H. Fu, Y. Cheng, *Curr. Org. Chem.* **2012**, *16*, 1423.
- [13] a) Z. Li, Y. Dong, B. Mi, Y. Tang, M. Häußler, H. Tong, Y. Dong, J. W. Y. Lam, Y. Ren, H. H. Y. Sun, K. S. Wong, P. Gao, I. D. Williams, H. S. Kwok, B. Z. Tang, *J. Phys. Chem. B* **2005**, *109*, 10061; b) A. J. Boydston, B. L. Pagenkopf, *Angew. Chem.* **2004**, *116*, 6496; *Angew. Chem. Int. Ed.* **2004**, *43*, 6336; c) X. Zhan, S. Barlow, S. R. Marder, *Chem. Commun.* **2009**, 1948; d) S. Li, T. Leng, H. Zhong, C. Wang, Y. Shen, *J. Heterocycl. Chem.* **2012**, *49*, 64.
- [14] S. Yamaguchi, R. Z. Jin, K. Tamao, *J. Organomet. Chem.* **1998**, *559*, 73.
- [15] a) J. Zhou, Z. Chang, Y. Jiang, B. He, M. Du, P. Lu, Y. Hong, H. S. Kwok, A. Qin, H. Qiu, Z. Zhao, B. Z. Tang, *Chem. Commun.* **2013**, 49, 2491; b) Z. Zhao, S. Chen, J. W. Y. Lam, Z. Wang, P. Lu, M. Faisal, H. H. Y. Sung, I. D. Williams, Y. Ma, H. S. Kwok, B. Z. Tang, *J. Mater. Chem.* **2011**, *21*, 7210.
- [16] a) W. Wu, S. Ye, R. Tang, L. Huang, Q. Li, G. Yu, Y. Liu, J. Qin, Z. Li, *Polymer* **2012**, *53*, 3163; b) B. He, S. Ye, Y. Guo, B. Chen, X. Xu, H. Qiu, Z. Zhao, *Sci. China Ser. B* **2013**, *56*, 1221.
- [17] a) L.-H. Zhang, T. Jiang, L.-B. Wu, J.-H. Wan, C.-H. Chen, Y.-B. Pei, H. Lu, Y. Deng, G.-F. Bian, H.-Y. Qiu, G.-Q. Lai, *Chem. Asian J.* **2012**, *7*, 1583; b) Z. Zhao, T. Jiang, Y. Guo, L. Ding, B. He, Z. Chang, J. W. Y. Lam, J. Liu, C. Y. K. Chan, P. Lu, L. Xu, H. Qiu, B. Z. Tang, *J. Polym. Sci. Part A* **2012**, *50*, 2265; c) Z. Zhao, Y. Guo, T. Jiang, Z. Chang, J. W. Y. Lam, L. Xu, H. Qiu, B. Z. Tang, *Macromol. Rapid Commun.* **2012**, *33*, 1074.
- [18] a) Y. Cao, I. D. Parker, G. Yu, C. Zhang, A. J. Heeger, *Nature* **1999**, 397, 414; b) M. Wohlgenannt, K. Tandon, S. Mazumdar, S. Ramaesha, Z. V. Vardeny, *Nature* **2001**, *409*, 494; c) C.-G. Zhen, Z.-K. Chen, Q.-D. Liu, Y.-F. Dai, R. Y. C. Shin, S.-Y. Chang, J. Kieffer, *Adv. Mater.* **2009**, *21*, 2425.

Received: August 19, 2013

Published online on January 8, 2014